GSA Data Repository 2017192

Lecumberri-Sanchez et al., 2017, Fluid-rock interaction is decisive for the formation of tung-sten deposits: Geology, doi:10.1130/G38974.1.

Appendix DR1. Detailed methods

The samples selected for this study belong to veins and corresponding wallrock collected over a vertical extent of 150 m and horizontal extent of over 2 km at the Panasqueira mine. The location of the samples for this study are shown in Fig. DR1.

Fluid inclusions associated with the tungsten mineralization stage were identified petrographically. These inclusions were predominately in secondary assemblages in quartz, and their relationship with tungsten precipitation can be demonstrated based on petrographic evidence of host quartz pre-dating wolframite (Fig. DR2), local association with small wolframite crystals along the same fracture as the fluid inclusions (Fig. DR2), and equal trace element ratios to fluid inclusions hosted in wolframite (Fig. DR2). Fluid inclusion microthermometry was done using a Linkam THS600 stage to determine the salinity and CO_2 content of the fluid, and in some cases to determine the homogenization temperature. Homogenization temperatures were not measured in all samples to prevent fluid inclusion decrepitation. Composition of fluid inclusions was determined by combining microthermometry (for the bulk salinity of the fluid) with a highly sensitive sector-field mass spectrometer (ELEMENT XR) coupled with a 193 nm excimer laser for LA-ICPMS analysis of the inclusions. Fluid inclusions petrographically related with wolframite mineralization have thermometric and compositional properties similar to many fluid inclusions occurring in quartz where the petrographic constraints are less clear. Potential post-entrapment modification issues have been evaluated based on consistency of thermometry and composition of fluid inclusions within fluid inclusion assemblages.

In Fig. 1, fluid inclusion assemblages where a given element had more than 1 fluid inclusion above detection limit are plotted as the average of concentrations and the error bars represent the standard deviation for all the fluid inclusions within the assemblage. The cupola, while unlikely to have generated all the fluids in the system, is generally accepted to have at minimum acted as a conduit for those fluids and therefore has been used as a center to evaluate proximal versus distal characteristics of the ore fluids. Limits of detection are a function of signal to background and therefore depend on the magnitude of the signal (size of the inclusion and fluid concentration) and on the background for a given element. Fluid inclusions assemblages where a given element was below detection limit for all fluid inclusions or for all fluid inclusions but one are reported as the minimum limit of detection for the fluid inclusion assemblage. Aluminium concentrations have a wider variability than other elements and some of the higher aluminium concentrations reported may be the result of micro inclusions of muscovite in the fluid inclusions analysed or of quartz refinement during maturation of the fluid inclusion shape (Lambrecht and Diamond, 2014). However, Al concentrations in the range of 70 to 150 ppm were consistent among multiple inclusions in one fluid inclusion assemblage and demonstrate significant Al mobility in the fluid, consistent with the abundance of micas and local topaz as vein minerals and the wall-rock reactions in

the main text. Fluid inclusion concentrations and thermometry are presented in *Appendix DR2. Fluid inclusion data*.

The variation of the chemical composition of the host rock as a function of distance from the vein was determined by XRF analysis. We cut 0.7 to 1 cm thick slabs parallel to the vein wall at progressive distances from the vein. Each of these slabs was crushed, ground in an agate mill and mixed with Cereox wax in a pressed pill that was then used to obtain bulk-rock composition as a function of distance from the vein (Halter and Williams-Jones, 1996). The results of these XRF analyses for a representative coarse grain schist (X) and fine grain schist (4A) are presented in *Appendix DR3. XRF data*.

Zr/Ti ratios remain constant throughout the transects perpendicular to the vein, indicating that these two elements are immobile during alteration. Therefore the enrichment and depletion of elements in the host rock from XRF data have been calculated based on a normalization to Zr and using the most distal slab of each transect (10 to 15 cm away from the vein) as reference sample approximating the unaltered local host rock. Note that, while the most distal sample belongs to the altered vein halo, the concentrations of elements in unaltered fine grain and coarse grain schist as reported by Polya (1989) plot in the same trend and indicate further enrichment/depletion for each element with respect to the unaltered rock. The normalizations to Zr and the enrichment/depletion calculated are presented in *Appendix DR3. XRF data*.

The minimum halo thickness (Z) required to produce a grade (G) in the vein considering an average iron loss in the halo ($X_{Fe2O3lost)}$ from the host rock is given by the equation:

$$Z=[G*X_{Fe/FeWO4}]/[2*\rho*X_{Fe2O3/rock}*X_{Fe/Fe2O3}*X_{Fe2O3lost}]$$

Where Z is the distance from the vein for which the average iron loss has been measured; G is the tungsten grade in kg $FeWO_4/m^2$; $X_{Fe/FeWO4}$ is the mass fraction of iron in ferberite; 2 is a factor to account for the alteration taking place in both sides of the vein; ρ is the rock density in kg/m^3; $X_{Fe2O3/rock}$ is the Fe_2O_3 mass fraction of the unaltered host rock; $X_{Fe/Fe2O3}$ is the mass fraction of Fe in Fe_2O_3; and $X_{Fe2O3lost}$ is the Fe_2O_3 mass fraction lost from the interval of host rock measured with respect to unaltered rock. Current grades at panasqueira oscilate around 5 Kg/m^2, where the grade units represent the mass of wolframite per square meter of vein in plan view (Fig DR2). The Beira schist at Panasqueira has an average ~6.5 wt % Fe_2O_3. Fig DR2 represents the minimum halo width for given average Fe_2O_3 loss from the schist based on these calculations. Note that, while wolframite also occurs in the host rock, wolframite precipitation in the host rock does not require iron mobilization and therefore has not been accounted for in this mass balance calculation.

Percentage of tungsten vein deposits and percent tungsten production from vein deposits hosted in metapelites worldwide was calculated based on the database compiled by Werner et al. (2014). Based on this database, around 70 % of W vein deposits worldwide are hosted exclusively in metasedimentary rocks (in addition to another 15% in the contact between the intrusive and the aureole). Furthermore, within tungsten vein deposits, the ones hosted exclusively in metasedimentary rocks produce over 75 % of the tungsten production worldwide (in addition to another 10 % from deposits in the contact between the intrusive and the aureole). Furthermore, where the composition of

wolframite is specified within the database, ferberite-dominated systems are always hosted in metasedimentary rocks. The data extracted from Werner et al. (2014) is provided in *Appendix DR4. Tungsten deposits worldwide*.

Fig DR1.

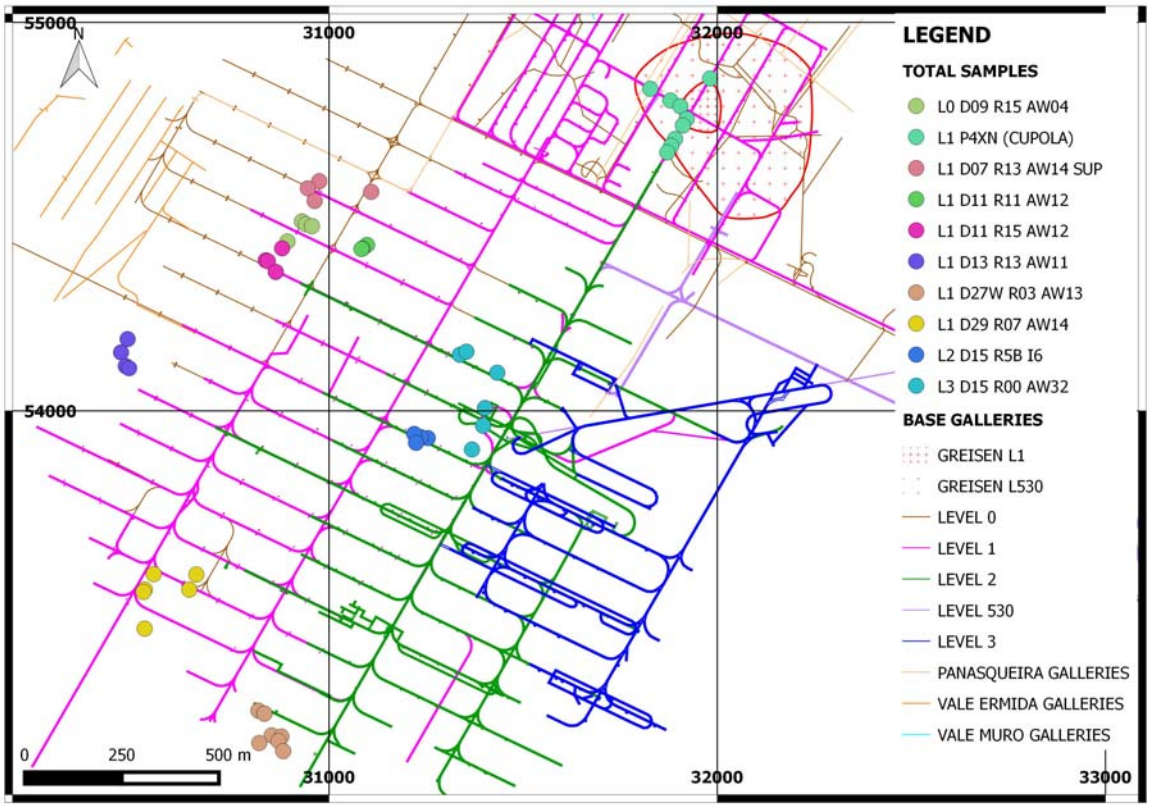

Fig DR1. Map projection of the Panasqueira mine with sample locations. Galleries in different colors represent the different main levels at the mine. The differences in elevation between levels are: 60 m between L0 and L1, 60 m between L1 and L2 and 90 m between L2 and L3 with intermediate levels every 10 m. Therefore for this study we have sampled over 2 km horizontal extent and over 100 m vertical extent.

Fig DR2

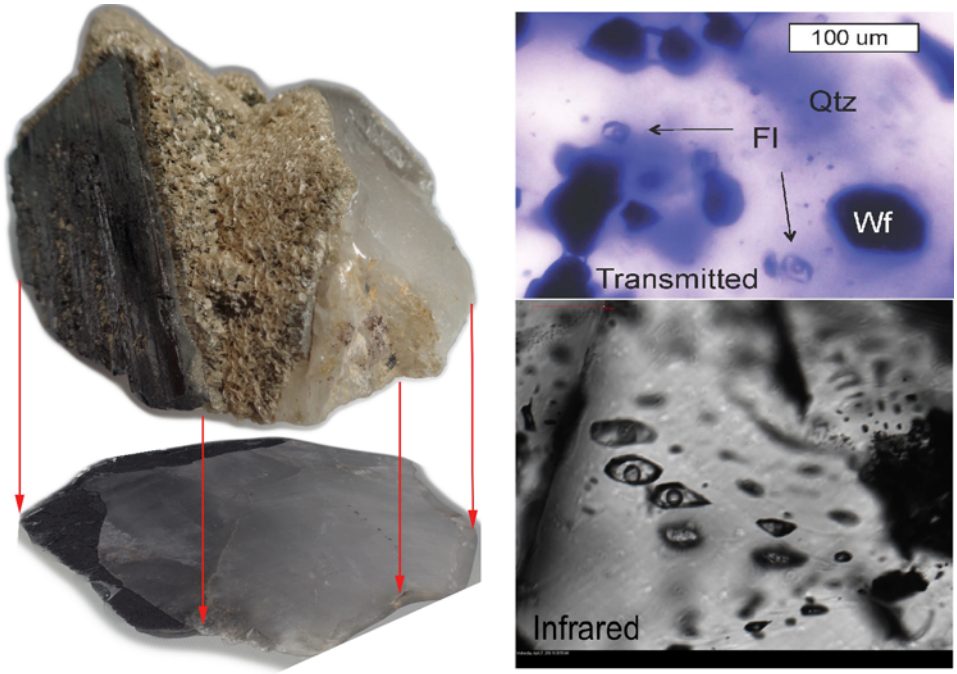

Fig DR2. Left: Hand sample evidence of quartz predating wolframite. Top right: photomicrograph under transmitted light of fluid inclusions associated with small wolframite crystals along the same fracture. Bottom right: photomicrograph of fluid inclusions in wolframite using an infrared camera and showing equivalent phase ratios as CO_2-bearing secondary fluid inclusion assemblages in quartz (note that element ratios of these fluid inclusions also coincide with many secondary fluid inclusion assemblages in quartz).

Fig DR3.

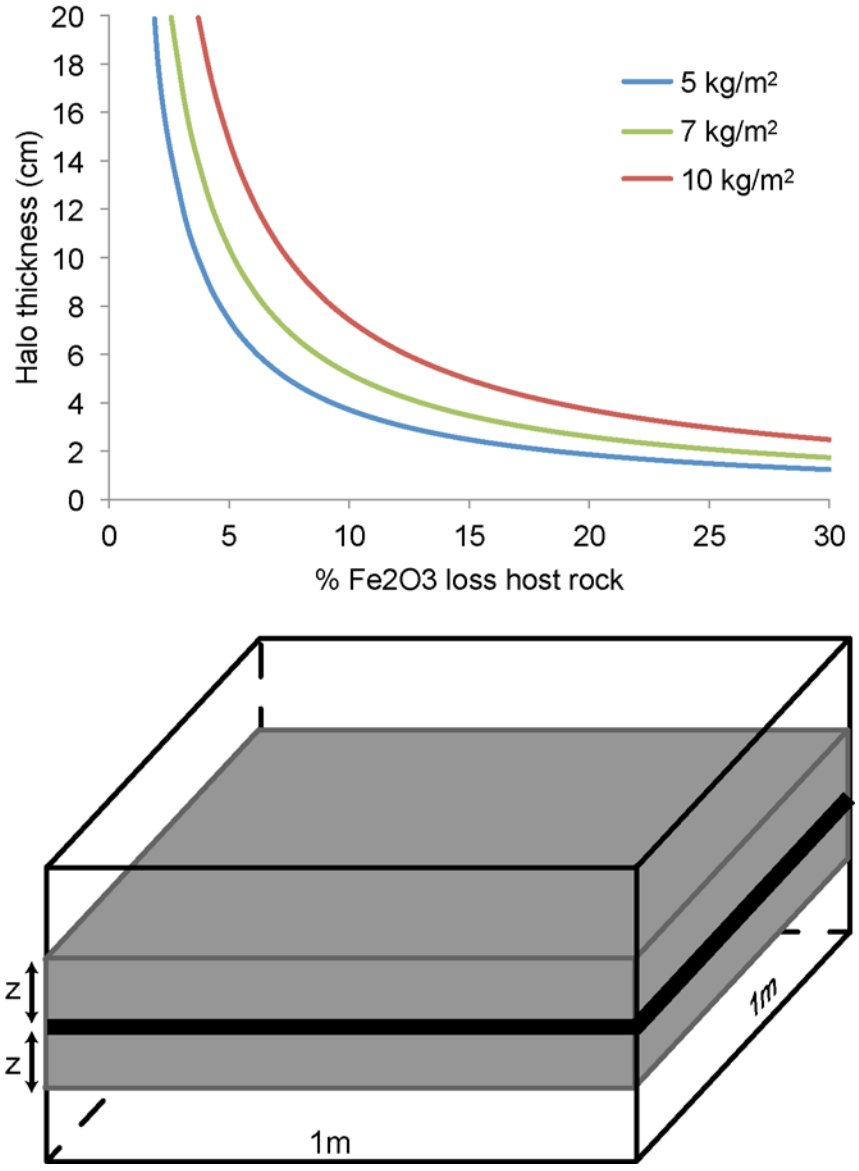

Fig DR3. Top: Minimum alteration halo thickness necessary to produce 5 kg/m^2 (blue line), 7 kg/m^2 (green line) and 10 kg/m^2 (red line) considering a given average Fe_2O_3 loss through the halo (x-axis). Bottom: Schematic representation of vein (thick black) and associated alteration halo (gray area). The grade unit "kg/m^2" correspond to the mass of wolframite in the vein volume represented in this diagram.

References for Appendix DR1

Halter, W. E., and Williams-Jones, A. E., 1996, The role of greisenization in cassiterite precipitation at the East Kemptville tin deposit, Nova Scotia: Economic Geology, v. 91, no. 368-385.

Lambrecht, G., and Diamond, L. W., 2014, Morphological ripening of fluid inclusions and coupled zone-refining in quartz crystals revealed by cathodoluminescence imaging: Implications for CL-petrography, fluid inclusion analysis and trace-element geothermometry: Geochimica et Cosmochimica Acta, v. 141, p. 381-406.

Polya, D. A., 1989, Chemistry of the main-stage ore-forming fluids of the Panasqueira W-Cu-(Ag)-Sn deposit, Portugal - implications for models of ore genesis Economic Geology, v. 84, no. 5, p. 1134-1152.

Werner, A. B. T., Sinclair, W. D., and Amey, E. B., 2014, International strategic mineral issues summary report- Tungsten: U.S. Geological Survey Circular, v. 903-O, p. 74.